



BRACE END FLEXIBILITY EFFECTS ON THE STABILITY OF BUCKLING RESTRAINED BRACED FRAME

S.Y. Vazquez-Colunga⁽¹⁾, C.L. Lee⁽²⁾, G.A. MacRae⁽³⁾

⁽¹⁾ Ph.D. Candidate, University of Canterbury, saul.vazquezcolunga@pg.canterbury.ac.nz

⁽²⁾ Senior Lecturer, University of Canterbury. chin-long.lee@canterbury.ac.nz

⁽³⁾ Professor, Tongji University & Associate Professor, University of Canterbury. gregory.macrae@canterbury.ac.nz

Abstract

This study investigates effects of column twisting and gusset plate (GP) buckling on the performance of a single storey buckling restrained braced (BRB) frame with pinned beam connections using finite element analysis. Column twist restraint is represented by the beam-column joint rotational stiffness $K_{y-joint}$ about the column axis at the top of the column. Frame performance is evaluated in terms of maximum frame lateral force, brace axial force, interstorey drift, and cumulative plastic deformation. Additional rotational stiffness was provided to the joint at the top of the column and by providing a slab. It was found that $K_{y-joint}$ required to prevent frame out-of-plane buckling under cyclic in-plane displacement was approximately five times the initial rotational stiffness. Greater column top rotational restraint was provided by the slab, so there was no buckling for this case.

Keywords: Gusset Plates; Buckling, Stability, Buckling Restrained Braces, Column Twisting.



1. Introduction

In New Zealand and around the world, buckling restrained braced frames (BRBFs) have become a popular system to resist seismic lateral load. They include a sub-system made of buckling restrained braces (BRBs) and gusset plates (GPs), and the remaining elements such as beams, columns, and slabs. For the BRBF to perform well during earthquakes, it is important for both the BRB-GP sub-system and the frame elements to be designed with all possible failure modes considered.

It is common to design each element of the BRBF independently neglecting the interaction between components. For example, GPs are designed as an equivalent column [1] using an effective length factor to account for the restraints provided by the connection zone, the brace and the frame elements. Recommendations are available for the definition of the effective length factor [2-5], although there is no single generally accepted value.

Recently, the importance of considering the stability of a BRBF as part of a BRB-GP sub-system [6-9] have become apparent. In some approaches, beam-column restraints are included as rotational springs, and the GP and its connection zone is a single element and the effect of all components contributing to brace end flexibility may not be explicitly acknowledged, and this can result in errors in estimating the system capacity.

One possible flexibility at a brace end is column flexural lateral torsional (FLT) buckling failure. This failure mode was observed during a moment resisting frame test [10, 11]. Zhang and Ricles [12, 13] suggested the use of a slab without a gap between column and slab to prevent column twisting. However, in practice, a gap is often provided between the concrete slab and the column to limit over strength effects [14], making this failure mode possible.

It may be seen from the discussion above that in order for good behavior there is a need for all effects contributing to the possibility of BRBF instability (e.g. columns, beams, braces, GPs and their connections) to be understood and considered in design. This paper seeks to address this need by seeking answers to the following questions for a finite element (FE) model of single storey braced frame subject to in-plane displacement.

1. Can frame instability from beam-column joint rotational stiffness be modelled?
2. How do the results compare with experimental tests?
3. Is it possible to prevent instability by choosing appropriate beam-column joint rotational stiffness?
4. Can the presence of a floor slab significantly prevent the likelihood of BRBF buckling?

2. BRBF Information

A single-bay one-story braced frame tested at the University of Canterbury is used for modelling in this study. The frame bay centerline width was 3.05m and its height 2.30m. The sections used for the frame elements were 150UC30.0 for the columns, 150UB18.0 for the top beam and 310UB40.4 for the foundation beams. The steel grade for beams, columns and plates was AS/NZS 3679.1 Grade 300. An additional 200x75 PFC channel beam was provided to increase the out-of-plane stiffness to the beam for all tests except BRBF-1. The channel had pinned-roller supports on one end to avoid adding lateral stiffness to the frame. The test setup and geometry can be seen in Bottom GP: plate dimensions and location of holes

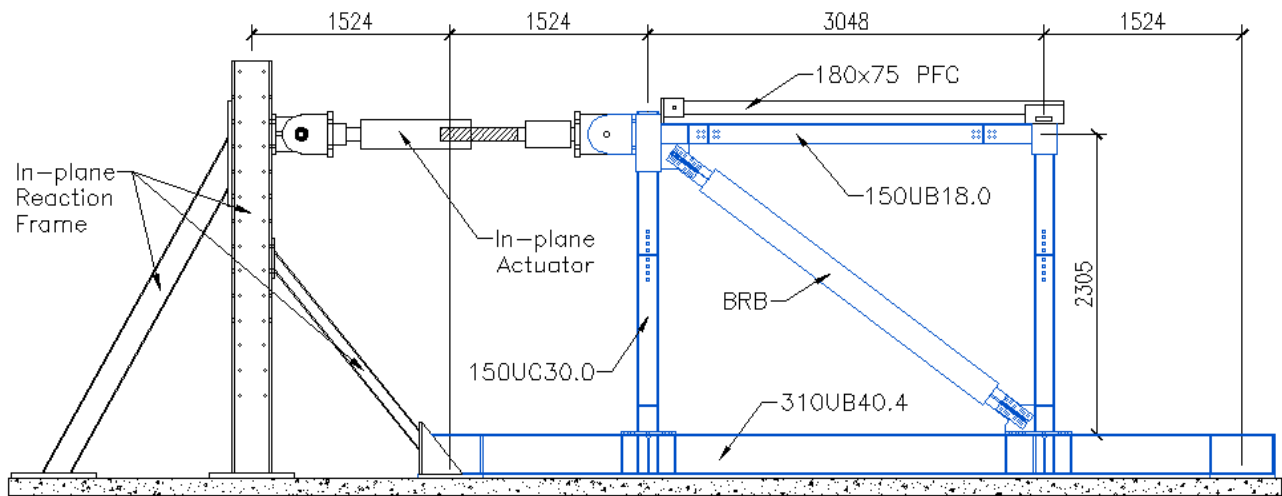
Fig. 1. Out-of-plane actuators at the column tops limit out-of-plane movement there.

Depending on the specimen tested, BRBs or stocky braces were used. The BRB yield strength P_y was 158kN, its tension strength T_{BRB} is 236kN based on the yield stress multiplied by the core area and an overstrength value of 1.50 estimated according to NZS3404 [15]. The compressive strength C_{BRB} is 272kN, which was taken as 1.15 times that of the tensile strength based on recommendations from the manufacturer. The BRB core had a 70x10mm rectangular section made of steel LYP225 (i.e. the nominal lower yield point is 225MPa) and the casing diameter was 203mm with a wall thickness of 8mm made of steel Q235. A stocky brace was made by welding the BRB end to the casing. This increased the brace yield strength P_y to 1152kN.

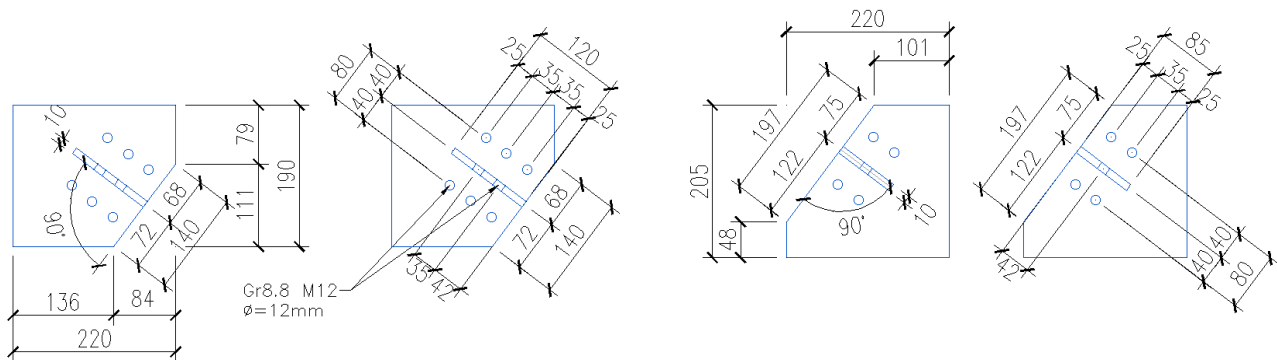


The top GP size was 220x190mm with a thickness (t_{gp}) of 10mm and a connection length (L_c) of 120mm as shown in Figure 4. The bottom GP size was 220x205mm with thicknesses of 5mm and 10mm and connection lengths of 120mm and 85mm. The BRB-to-GP connection was made using Grade 8.8 bolts with a diameter of 12mm and splice plates with a thickness of 6mm. For this study, attention will be focused on three of the tested specimens: BRBF-1, BRBF-9 and BRBF-11. The specimen details can be seen in Bottom GP: plate dimensions and location of holes

Fig. 1 and Table 1. The stiffener mentioned in Table 1 is a continuation of that on the BRB end zone, attached to the gusset plate over the length of overlap of the BRB connection. It is shown in Figs. 2a and 2b, but is not present in Fig. 2c.



a) Test Elevation



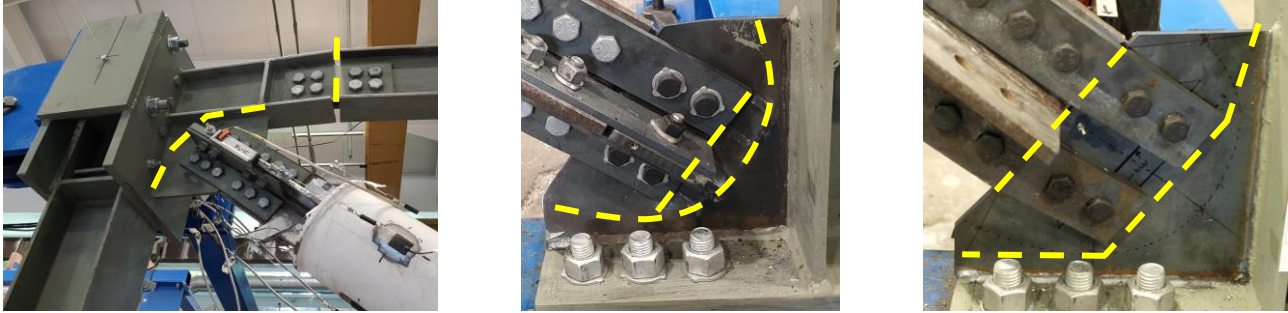
b) Top GP: plate dimensions and location of holes

c) Bottom GP: plate dimensions and location of holes

Fig. 1 – Experimental Test Setup and GP Geometry

Table 1 – Specimen Details

Specimen ID	Buckling Mechanism	Brace Type	t_{gp} (mm)		L_c (mm)		Stiffened	
			Top	Bottom	Top	Bottom	Top	Bottom
BRBF-1	Column FLT + GP	BRB	10	10	120	120	Yes	Yes
BRBF-9	GP-GP	Stocky	10	5	120	85	Yes	Yes
BRBF-11	End Zone-GP	Stocky	10	5	120	85	Yes	No



a) BRBF-1: column FLT buckling b) BRBF-9: GP local sway buckling c) BRBF-11: GP buckling

Fig. 2 – Test Specimen Observed Buckling

For a buckling mechanism, three hinges are required over the extended brace region. At the ends not shown, a single flexural yield line occurred in the GP for all cases. The three buckling modes are different. Only in BRBF-1 did column FLT buckling contribute to the deformation. The buckling modes in BRBF-9 and BRBF-11 were affected by the presence of the stiffener. The gusset plate thicknesses were the same for these two details.

3. Methodology

3.1 Column Rotational Stiffness Considerations

The out-of-plane movement at the top of the column is restrained at the column centerline due to the out-of-plane actuators. Here, the resistance to rotation at the top of the column includes the resistance provided by the column (in warping and St Venants torsion), by the beam (but this component is small as it is pinned on the web), by the brace, and by the channel member when it is provided for BRBF-9 and BRBF-11. The buckling is initiated by the force applied by the in-plane loading ram.

The resistance of the top of the column to twist (i.e. rotation about the vertical y -axis) is called $K_{y,joint}$ and is represented by a rotational spring at the top of each column as shown in Fig. 3. Here, the column warping is prevented at the top and bottom, and the column, brace, beam and channel torsional stiffness about the centre of the column was found using the finite element computer software Abaqus [16] to obtain rotational stiffnesses $K_{y,column}$, $K_{y,brace}$, $K_{y,beam}$ and $K_{y,channel}$ respectively. The parameters in Eqn. (1) are normalized by the brace stiffness, $K_{y,brace}$, where, for example, α_{column} is equal to K_{column}/K_{brace} , and similarly for the other stiffnesses. The total rotational stiffness about the centre of the column is α_{total} times that of the brace alone. It is noted here that (i) $\alpha_{brace} = 1$, (ii) in calculating $K_{y,column}$ the bolted column splice was ignored for simplicity, and (iii) $K_{y,beam}$ considers the presence of the splices.

$$\begin{aligned}
 K_{y,joint} &= K_{y,column} + K_{y,brace} + K_{y,beam} + K_{y,channel} \\
 &= \alpha_{column} K_{y,brace} + \alpha_{brace} K_{y,brace} + \alpha_{beam} K_{y,brace} + \alpha_{channel} K_{y,brace} \\
 &= (\alpha_{column} + \alpha_{brace} + \alpha_{beam} + \alpha_{channel}) K_{y,brace}
 \end{aligned} \tag{1}$$

$$K_{y,joint} = \alpha_{total} K_{y,brace} \tag{2}$$

Cases analyzed include:

- (i) no effective slab (i.e. $\alpha_{channel} = 0$, and $K_{y,joint} = (\alpha_{column} + \alpha_{brace} + \alpha_{beam}) K_{y,brace}$).
- (ii) the effective stiffness of the channel provided ($\alpha_{column} + \alpha_{brace} + \alpha_{beam} + \alpha_{channel}$), and
- (iii) the presence of a stiff floor slab restraining all rotation at the column centerline (i.e. $\alpha_{channel}$ and $K_{y,joint}$ tends to infinity).



Using the properties of the beam, brace and column used during the test, the normalized rotational stiffness α_{beam} , α_{brace} and α_{column} are 4.1, 1.0 and 0.7, respectively, and, the brace stiffness $K_{y,brace}$ is equal to 7.2 kN-m/rad. The frame stability was evaluated in terms of the maximum frame lateral force (F), brace axial force (N) and interstorey INP drift when the brace was in compression. To evaluate the BRB performance, the cumulative plastic deformation (CPD) was calculated until the moment instability was observed.

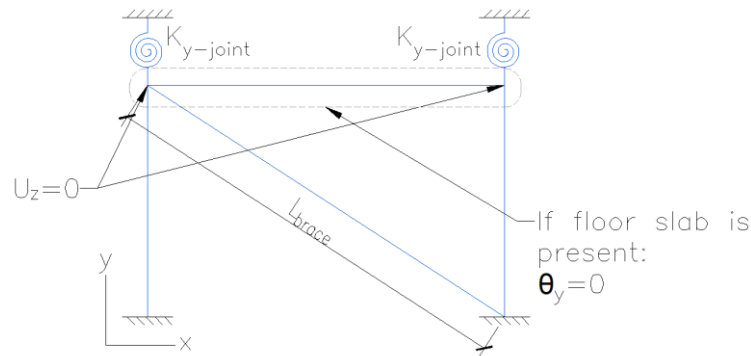


Fig. 3 – Beam-Column Joint Rotational $K_{y-joint}$

3.2 Loading Protocol

The loading protocol used for the study of $K_{y-joint}$ is similar to the recommended by the AISC Specification [2]. It was modified to reach a maximum drift of 2.5% instead of 2.0%. After reaching this maximum drift, 10 additional cycles with a constant drift amplitude of 2% were applied. As a reference, completing this full loading protocol without instability implies a CPD of 1050, while the minimum CPD required by the AISC Specification is 200.

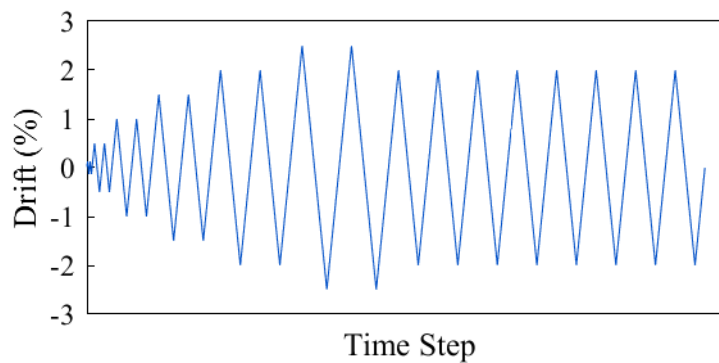


Fig. 4 – Loading Protocol used for stability analysis

3.3 Description of numerical models

The numerical analysis was performed using FE models and the finite element computer software Abaqus 2017 [15]. Shell elements were used to model beams, columns, gusset plates, and splice plates at the connections and brace ends. For models when a BRB is used, it was modelled using two beam elements: one for the core and one for the casing. Both core and casing were coupled along all degrees of freedom except that along the BRB longitudinal axis. When a stocky brace was used, the BRB core was removed and the casing was modelled using shell elements. Contact between elements was included and bolts were modelled as rigid connectors. The base of both column were fully restrained against translation and rotation and the beam-column joints restrained against out of plane translation. The displacements from the loading protocol were applied at the left beam-column joint. The general model details can be seen in Fig. 5.

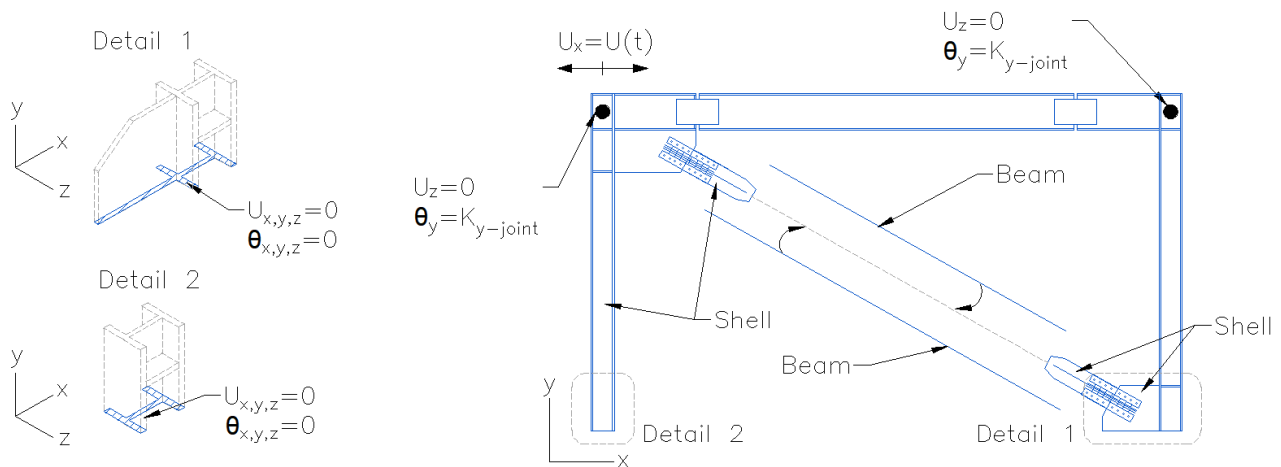


Fig. 5 – General Details and Assumptions for the FE models

The materials assigned to each element were defined depending on the steel grade used during the test. For the hysteretic behavior, a bilinear kinematic hardening for the stress-strain relationship was used. Material fatigue was not included on the material definition, in order to remove fracture as a possible failure mechanism.

4. Results

4.1 Model calibration

For the calibration stage, the same loading protocol applied during tests was used on the FE analysis. The calibration results of all specimens can be seen in Table 2. The forces shown are the maximum forces obtained. These are the same as that at the initiation of buckling as this caused the mechanism and sudden strength decrease.

Table 2 – Comparison of Experimental versus Numerical Behaviour

Specimen ID	Frame force, F (kN)			Brace Force, N (kN)			Frame Interstorey Drift (%)		
	Test	FE	(FE/Test-1)	Test	FE	(FE/Test-1)	Test	FE	(FE/Test-1)
BRBF-1	316	208	-34.2%	245	175	-28.6%	1.05	1.09	+3.8%
BRBF-9	334	346	+3.6%	315	291	-7.6%	0.52	0.56	+7.7%
BRBF-11	276	296	+7.2%	266	245	-7.9%	0.52	0.60	+15.4%

The FE results for specimens BRBF-9 and 11 were within $\pm 8\%$ those obtained from the test. The FE results were sometimes positive indicating that the FE model strength was greater than the experimental strength. In this case, the FE model was non-conservative possibly because initial out-of-straightness and residual stresses were not included in the model. However, for the case of specimen BRBF-1, with the column FLT buckling, the frame lateral strength was 34.2% less than obtained from test. A reason for this may be that the FE model assumed sliding of the core within the casing, but for this BRBF-1 brace, the quality control was poor and there was significantly more compression strength than expected being more than 1.5 times the peak tensile strength. Fig. 6a and b show that the finite element deformations are consistent with that obtained in the experiment. For BRBF-9, the FEM hysteresis loop matches that from the experiment well as seen in Fig. 7c. To identify the moment when GP buckling initiated, the brace axial force, N , and the out-of-plane deformation at the tip of the bottom GP were measured. When the GP tip out-of-plane deformation rapidly increases with no increment on the brace axial force, instability has been reached



and this brace axial force is the GP buckling load. Fig. 7d shows the brace axial force versus GP tip out-of-plane deformation obtained from test and FE analysis for BRBF-1. Here, the FE analysis aborted when the deformations became large at a maximum brace axial force of 291kN, 7.6% smaller than that obtained from test.

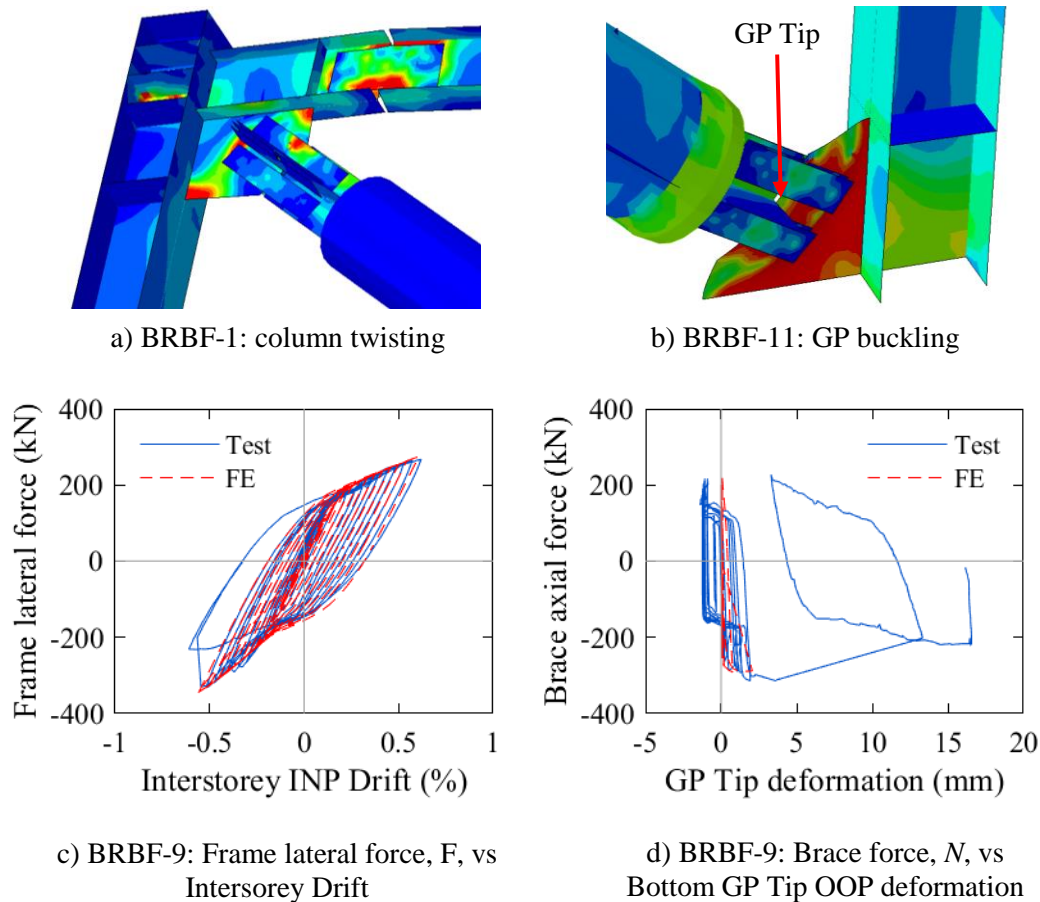


Fig. 6 – FE analysis calibration results

4.2 Influence of $K_{y-joint}$ on system stability

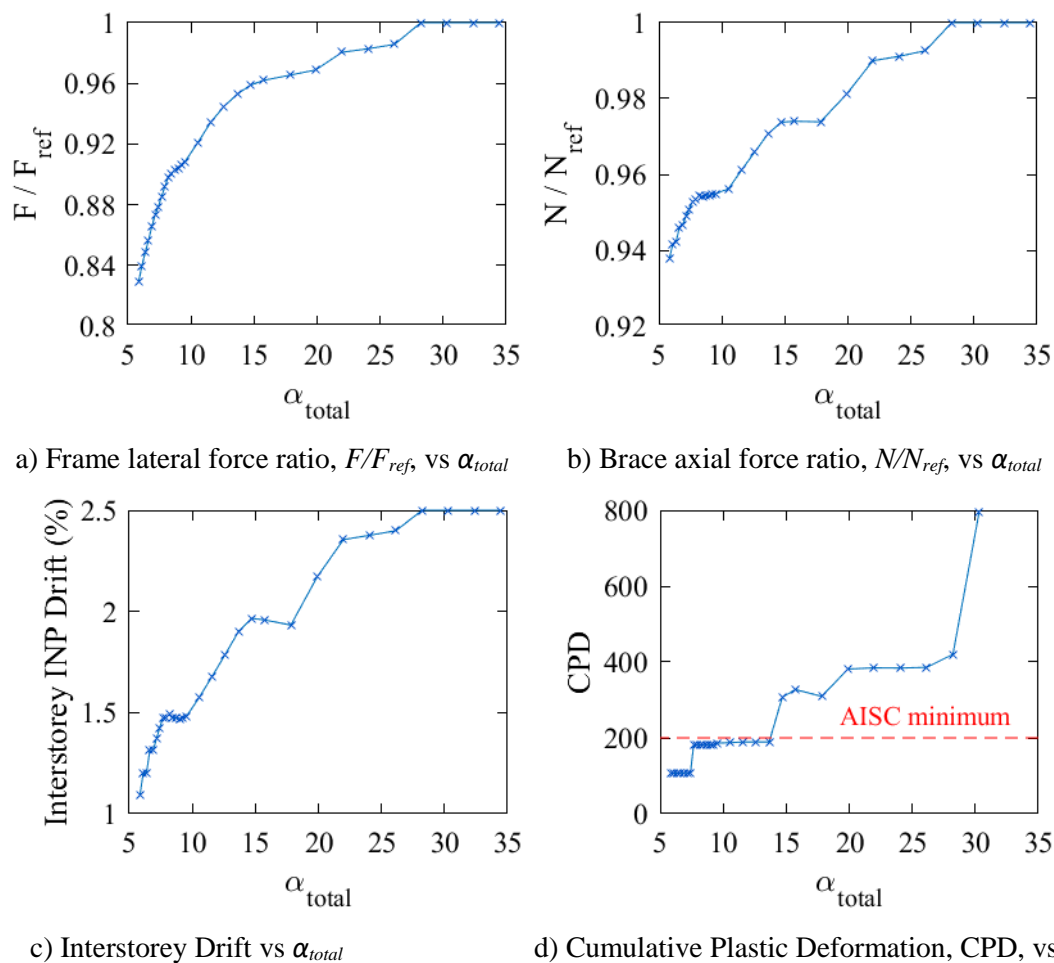
For BRBF-1, column FLT buckling occurred when there was no extra slab torsional resistance (i.e. when $\alpha_{channel} = 0$). When the beam-column joint rotation was restrained by the channel, and by the slab, the analysis remained stable. Maximum values of F and N did not vary with $\alpha_{channel}$ for these cases. Also there was no GP buckling in these cases as all inelasticity occurred by yielding of the core. These F and N values were used as references to normalize the results from each analysis. The reference frame lateral force F_{ref} is 251kN, and the brace axial force N_{ref} is 187kN.

The frame stability improved when $\alpha_{channel}$ was increased. Initially at $\alpha_{channel} = 0$ (i. e. at $\alpha_{total} = 5.8$), all performance evaluators were not satisfactory. Once $\alpha_{channel}$ increased to 14.7, the calculated CPD was larger than the minimum of 200, but F , N , and the interstorey drift were still less than the reference ones. When increasing α_{total} to 20.3, both frame and brace forces, F and N , and the CPD were satisfactory, but the interstorey drift did not reach the maximum. It was not until $\alpha_{channel}$ increased up to 22.4 that all performance evaluators reached acceptable values. When $\alpha_{channel}$ is 22.4, the total normalized stiffness α_{total} is 28.2, the calculated CPD was larger than 200 and additionally, F , N , and the interstorey INP drift were equal to the reference ones. Therefore, a minimum normalized rotational stiffness $\alpha_{total-min} = 28.2$ is needed for the system to be stable. Several $\alpha_{channel}$ and α_{total} values of interest can be seen in Table 3.

Table 3 – Effect of Beam Restraint, $\alpha_{channel}$

$\alpha_{channel}$	α_{total}	Condition	F/F_{ref}	N/N_{ref}	Drift	CPD
0.00	5.8	Unstable	0.95	0.97	1.9 %	189
8.8	14.6	Unstable	0.96	0.97	2.0 %	307
20.3	26.1	Unstable	0.99	0.99	2.4 %	386
> 22.4	> 28.2	Stable	1.0	1.0	2.5 %	>386

The frame lateral force, F , increased rapidly until α_{total} was equal to 15, after it, the increment rate decreased until there was no increment at $\alpha_{total} > 28.2$. For the brace axial force, N , and the interstorey drift, the increment rate followed a similar trend up to $\alpha_{total} = 28.1$, with no increment observed after this value. Regarding the cumulative plastic deformation, CPD, for α_{total} values between 7.6 and 13.6, it ranged from 182 to 189, and suddenly increased to 307 once α_{total} was equal to 14.7. The reason is that when $\alpha_{total} = 14.7$, $K_{y-joint}$ is large enough to allow the frame to complete more cycles of the loading protocol, and, therefore, increase the brace CPD. A similar sudden increment can be observed at $\alpha_{total} = 28.2$, where the frame was able to complete additional cycles. The variation of F , N , interstorey drift and CPD versus the increment of α_{total} is shown in Fig. 8.

Fig. 7 – Variation of frame stability due to α_{total}



For comparison, when $\alpha_{channel}$ is 0 (frame tested without additional rotational stiffness), α_{total} is 5.8, which is approximately 5 times smaller than $\alpha_{total-min} = 28.2$. Additional rotational stiffness can be provided to each beam-column joint using a channel, other members, or a slab. For example, for the case of a joint which is part of a 3D structure without a slab, with four beams and two columns (one above and one below) framing into one joint, the total rotational stiffness can be computed. If α_{beam} is 4.1, α_{column} is 0.7 and α_{brace} is 1.0 say, α_{total} will be equal to $4\alpha_{beam} + 2\alpha_{column} + \alpha_{brace}$ equal to 18.8. This is 1.5 times smaller than $\alpha_{total-min}$, so column FLT buckling can be expected. Therefore, other restraints may be required. For example, it may be necessary to make the beams continuous (i.e. remove the pins), or provide a slab with sufficiently large rotational restraints to obtain stable behavior. It should also be noted that, to account for uncertainty in practice, a value of rotational restraint sufficiently greater than the minimum theoretical value is desirable.

5. Conclusions

This paper describes a study of the stability of a single storey braced frame with gusset plates and pinned beam connections using finite element analyses. The frame numerical behaviour, with three different configurations, was compared with experimental results where both column flexural lateral torsional (FLT) buckling and gusset plate (GP) buckling modes were observed. It was found that:

1. A simple model was created using the computer software ABAQUS which was able to model both instability resulting from gusset plate buckling and beam-column out-of-plane rotation.
2. Results of the analyses, which did not consider residual stresses or any initial out-of-straightness, were able to capture both modes of instability. When compared with the results of 3 experimental tests where instability occurred, the peak experimental frame strength obtained was between -7% (non-conservative) and 34% (conservative) of that from the analyses. In most cases, the strength was conservatively predicted.
3. Under loads as high as those that could be generated by the BRB brace, (i) when the beam-column joint rotational stiffness about the vertical axis was greater than 5 times that provided by the column, beam and brace (which was dominated by the column), there was no analysis instability when the GP was stiff, and (ii) when the beam-column joint rotational stiffness about the vertical axis was high, GP buckling was avoided.
4. The presence of a floor slab effectively limited the possibility of BRBF column flexural lateral torsional (FLT) buckling under the maximum BRB brace force.

4. Acknowledgements

The authors wish to thank the Heavy Engineering Research Association and the Department of Civil and Natural Resources Engineering at the University of Canterbury for their support to conduct part of the work done for this paper. The first author is also grateful to the National Council of Science and Technology of Mexico (CONACyT) for the scholarship received for the completion of his postgraduate studies. UC PhD candidate Jian Cui was involved at all stages of the experimental test program and his contributions are gratefully acknowledged.

5. References

- [1] Thornton WA (1984): Bracing connections for heavy construction. *Engineering Journal*, **21**(3), 139-148.
- [2] AISC Committee (2010): Specification for structural steel buildings (ANSI/AISC 360-10). American Institute of Steel Construction, Chicago-Illinois, USA.
- [3] Dowswell B (2006): Effective length factors for gusset plate buckling. *Engineering Journal*, American Institute of Steel Construction, **43**(2), 91.
- [4] Dowswell, B. (2014): Gusset Plate Stability Using Variable Stress Trajectories. *Structures Congress 2014*, Boston, USA.



- [5] Tsai KC, Hsiao PC (2008): Pseudo-dynamic test of a full-scale CFT/BRB frame—Part II: Seismic performance of buckling-restrained braces and connections. *Earthquake Engineering & Structural Dynamics*, **37**(7), 1099-1115.
- [6] Takeuchi T, Ozaki H, Matsui R, Suctu F (2014): Out-of-plane stability of buckling-restrained braces including moment transfer capacity. *Earthquake Engineering & Structural Dynamics*, **43**(6), 851-869.
- [7] Takeuchi T, Matsui R, Mihara S (2016): Out-of-plane stability assessment of buckling-restrained braces including connections with chevron configuration. *Earthquake Engineering & Structural Dynamics*, **45**(12), 1895-1917.
- [8] Westeneng B, Lee C-L, MacRae G, Jones A (2017): Out-of-plane buckling behaviour of BRB gusset plate connections. *Proceedings of 16th World Conference on Earthquake Engineering*, Santiago, Chile.
- [9] Zaboli B, Clifton C, Cowie K (2018): BRBF and CBF gusset plates: Out-of-plane stability design using a simplified Notional Load Yield Line (NLYL) method. *SESOC Journal*, **31**(1), 64.
- [10] Uang C-M, Ozkula G, Chansuk P (2019): Research on seismic design of deep wide-flange steel columns in the US. *12th Pacific Structural Steel Conference*, Tokyo, Japan.
- [11] Chi B, Uang C-M (2002): Cyclic response and design recommendations of reduced beam section moment connections with deep columns. *Journal of Structural Engineering*, **128**(4), 464-473.
- [12] Zhang X, Ricles JM (2006): Experimental evaluation of reduced beam section connections to deep columns. *Journal of Structural Engineering*, **132**(3), 346-357.
- [13] Zhang X, Ricles JM (2006): Seismic behavior of reduced beam section moment connections to deep columns. *Journal of Structural Engineering*, **132**(3), 358-367.
- [14] MacRae GA, Clifton GC (2015): NZ research on steel structures in seismic areas. *8th International Conference on Behavior of Steel Structures in Seismic Areas*, Shanghai, China.
- [15] SNZ, S. S. S. (2007): NZS 3404: 1997. *Standards New Zealand*, Wellington, New Zealand.
- [16] Dassault Systemes (2016): Abaqus/CAE 2017. Dassault Systemes Simulia Corp., Rhode Island, USA.